BPB Reports

Regular Article

Time-Dependent Regulation of DAMP Signaling: Differential Release of HMGB1 and RPL9 by Distinct Cell Death Pathways

Masahiro Watanabe,[a] Takao Toyomura,[a] Yasuko Tomono,[a] Hidenori Wake,[b] Takashi Nishinaka,[b] Hideo Takahashi,[b] Masahiro Nishibori,[c] and Shuji Mori[a,*]

[a]*Department of Pharmacology, School of Pharmacy, Shujitsu University, Okayama 703-8516, Japan;* [b]*Department of Pharmacology, Faculty of Medicine, Kindai University, Osaka-Sayama 589-8511, Japan;* [c]*Department of Translational Research and Drug Development, Okayama University Graduate School of Medicine, Dentistry, and Pharmaceutical Sciences, Okayama 700-8558, Japan*

Received February 25, 2026; Accepted March 19, 2026

High mobility group box 1 (HMGB1) is a critical pro-inflammatory damage-associated molecular pattern (DAMP), and ribosomal protein L9 (RPL9) has been identified as a potential "regulatory DAMP" that can suppress HMGB1's activity. However, it is unclear how pro-inflammatory DAMP signaling is initiated when these opposing molecules are released together. We hypothesized that the release kinetics of HMGB1 and RPL9 are differentially regulated depending on the cell type. To test this, we compared the release of HMGB1 and RPL9 from human macrophage (THP-1), liver (HepG2), and endothelial (EA.hy926) cell lines following stimulation with lipopolysaccharide and nigericin. In THP-1 macrophages, classical pyroptosis induced a rapid, sequential release of HMGB1 followed by RPL9. In contrast, HepG2 cells showed slower, apoptosis-like cell death, and RPL9 was released several hours before HMGB1. EA.hy926 cells were highly resistant to the stimulus. Notably, RPL9 release was closely associated with phosphatidylserine externalization in both THP-1 and HepG2 cells, regardless of their primary cell death pathway. Our findings demonstrate that the balance between pro-inflammatory and regulatory DAMPs is governed by a complex, cell-type-specific temporal control system intrinsically linked to the mode of cell death. Furthermore, we propose the existence of a novel, selective release pathway for RPL9. A deeper understanding of this time-dependent regulation may contribute to the development of new therapeutic strategies for inflammatory diseases.

Key words damage-associated molecular patterns, high mobility group box 1, ribosomal protein l9, pyroptosis, cell death

INTRODUCTION

High mobility group box 1 (HMGB1) is a representative damage-associated molecular pattern (DAMP) protein.[1)] DAMPs are endogenous molecules released from cells in response to tissue injury or stress.[2)] These molecules signal danger to the immune system and can induce an inflammatory response even in the absence of a pathogen, a phenomenon known as sterile inflammation. Sterile inflammation is now recognized as a key contributor to the pathogenesis of many non-infectious diseases, including autoimmune disorders, metabolic syndromes, and neurodegenerative diseases.[3)] HMGB1, typically a nuclear protein, is released from host cells and plays a critical role in initiating and amplifying inflammatory responses by stimulating pattern-recognition receptors such as the receptor for advanced glycation endproducts (RAGE) and toll-like receptors (TLRs).[4)] HMGB1 also enhances the effects of other pro-inflammatory molecules, such as lipopolysaccharide (LPS), which is a representative pathogen-associated molecular pattern (PAMP), and/or advanced glycation endproducts (AGEs).[5,6)] Despite extensive research, many aspects of HMGB1's function and regulatory mechanisms remain unclear.

We previously found that ribosomal protein L9 (RPL9), a known ribosomal constituent, is released from physically disrupted cells, similar to HMGB1, and is detectable in the serum of endotoxemia model mice.[7)] These findings suggest that RPL9 also functions as a DAMP. However, unlike HMGB1, when administered to cells with LPS, RPL9 did not enhance the effect of LPS. Notably, when all three molecules (LPS, HMGB1, and RPL9) were administered to macrophage cells, the enhancing effect of HMGB1 on LPS was abrogated by RPL9, suggesting a suppressive role for RPL9. Thus, RPL9 may belong to a novel category of molecules, which we refer to as "regulatory DAMPs," that modulate the effects of known DAMPs such as HMGB1.

*To whom correspondence should be addressed. e-mail: morimori@shujitsu.ac.jp

Based on these findings, if RPL9 is simultaneously released with HMGB1, then HMGB1's pro-inflammatory effects may be abolished from the beginning. This led us to question whether the release mechanism and timing of RPL9 differ from those of HMGB1.

The release of DAMPs, such as HMGB1, is a complex process that can be broadly categorized as active secretion from viable cells or passive release from dying cells.[8] Active secretion is a regulated process in which molecules like HMGB1 are transported from the nucleus to the cytoplasm and subsequently released through unconventional secretory pathways, often without the loss of cell viability. In contrast, passive release occurs when the plasma membrane is ruptured, allowing intracellular contents to leak out. This can occur through unregulated cell death, such as necrosis, which results from severe injury, but it can also occur through various forms of regulated cell death involving lytic steps. One key example of such a pathway is pyroptosis, an inflammatory form of programmed cell death triggered by inflammatory caspases such as caspase-1. This process involves the formation of a membrane-disrupting pore by caspase-cleaved gasdermin D (GSDMD). This pore facilitates the rapid release of pro-inflammatory cytokines, such as IL-1β and IL-18, which leads to cell lysis, resulting in the passive release of DAMPs, like HMGB1.[9,10] Pyroptosis is a critical host defense mechanism against bacterial infection.[11,12] To experimentally mimic this pathological state, where cells are exposed to pathogen-associated molecular patterns (PAMPs), the combined stimulation with bacterial endotoxin (LPS) and the potassium ionophore nigericin (NIG) is widely utilized as a robust model of inflammatory cell death.

In the present study, to determine whether the release mechanism and timing of RPL9 differ from those of HMGB1, we compared the release kinetics of the two proteins from THP-1 cells, a human macrophage model, investigating their release under pyroptosis-inducing conditions. Furthermore, we examined whether this stimulus prompts the release of HMGB1 and RPL9 in other cell types, namely HepG2 and EA.hy926 cells. Our results revealed distinct patterns of protein release across the three different cell lines, suggesting that these differences reflect the specific roles of various cell types and tissues in the regulation of inflammatory responses during infection *in vivo*, as discussed in detail in this study.

MATERIALS AND METHODS

Cell Culture and Sample Preparation THP-1 (JCRB, Osaka, Japan), HepG2 (JCRB, Osaka, Japan), and EA.hy926 (ATCC, Manassas, VA, USA) cells were grown in Roswell Park Memorial Institute 1640 medium, low-glucose Dulbecco's modified Eagle's medium (Nacalai Tesque, Kyoto, Japan), and high-glucose Dulbecco's modified Eagle's medium (Nacalai Tesque, Kyoto, Japan), respectively, supplemented with 10% fetal calf serum at 37°C in a humidified atmosphere containing 5% CO_2. For differentiation into macrophage-like cells, THP-1 cells were treated with 100 nM phorbol-12-myristate-13-acetate (PMA; Cell Signaling Technology, Danvers, MA, USA) for 16 h. The cells were then stimulated with 100 ng/mL LPS (FUJIFILM Wako, Osaka, Japan) and 10 μM NIG (FUJIFILM Wako, Osaka, Japan). The culture medium and cells were collected at 1, 6, and 24 h after stimulation. The culture medium was centrifuged at 300 × g for 5 min to remove cell debris. Subsequently, the supernatant was recovered and centrifuged at 2,000 × g for 30 min. The resulting supernatant was mixed with four volumes of cold acetone and precipitated at –80°C overnight. The precipitate was collected by centrifugation at 12,000 × g for 10 min, resuspended in Western blotting sample buffer, and sonicated.

Western Blotting Western blotting was performed according to a previously described procedure[13] using anti-HMGB1 (produced in our laboratory[14]), anti-RPL9 (Abcam, Cambridge, UK), or anti-GSDMD (Cell Signaling Technology, Danvers, MA, USA) antibodies. Recombinant HMGB1 and RPL9 were prepared as previously described.[7] Samples were loaded based on equal protein amount (25 μg for cell lysates) or equal volume (20 μL for culture supernatants). Loading consistency was verified by staining the membranes with Coomassie Brilliant Blue (CBB) solution (0.25% CBB R-250, 50% methanol, 10% acetic acid) (Supplementary Figs. 1–4).

Cellular Viability Assay Cell viability was assessed using the 3-(4,5-dimethylthiazol-2-yl)-5-(3-carboxymethoxyphenyl)-2-(4-sulfophenyl)-2H-tetrazolium, inner salt (MTS) assay with the CellTiter 96 AQueous One Solution Cell Proliferation Assay kit (Promega, Madison, WI, USA) according to the manufacturer's protocol. Briefly, cells were stimulated with LPS and NIG for 1, 6, or 24 h, and then the assay reagent was added to each well. After 3 h of incubation, the absorbance at 492 nm was measured using an MTP-320 microplate reader (CORONA ELECTRIC, Hitachinaka, Japan).

Cell Death Pattern Analysis The externalization of phosphatidylserine (PS) and the exposure of nuclear DNA were analyzed using the RealTime-Glo Annexin V Apoptosis and Necrosis Assay kit (Promega, Madison, WI, USA) according to the manufacturer's protocol. Briefly, cells were treated with the kit reagents and then stimulated with LPS and NIG for 24 h. Luminescence and fluorescence signals (excitation at 485 nm and emission at 530 nm) were measured at 1, 2, 3, 6, 20, 21, 22, and 24 h after stimulation using a Varioskan Lux microplate reader (Thermo Fisher Scientific, Waltham, MA, USA).

Statistical Analysis Statistical analysis among multiple groups was performed using Dunnett's test using R (version 4.4.3, The R Foundation for Statistical Computing, Vienna, Austria). *P*-values < 0.05, 0.01, or 0.001 were considered statistically significant. All data were presented as the mean ± standard error.

RESULTS

Time-Course Analysis of the HMGB1 and RPL9 Release from LPS and NIG-Stimulated Cells To compare the release kinetics of HMGB1 and RPL9, we utilized PMA-differentiated THP-1 cells, a human macrophage model. We adopted a co-stimulation protocol with LPS and nigericin to induce HMGB1 release. In this model, at 1 h after stimulation, HMGB1 was detected in the culture supernatant (Fig. 1). The amount of HMGB1 increased up to 6 h after stimulation, and slightly decreased by 24 h. RPL9 exhibited a similar pattern of increase and decrease, but the extent differed from that of HMGB1. Using 100 ng of recombinant HMGB1 and RPL9 as a reference, the amount of RPL9 was lower than that of HMGB1 at 1 h, comparable at 6 h, and almost undetectable at 24 h.

To assess potential differences between cell lines, HepG2

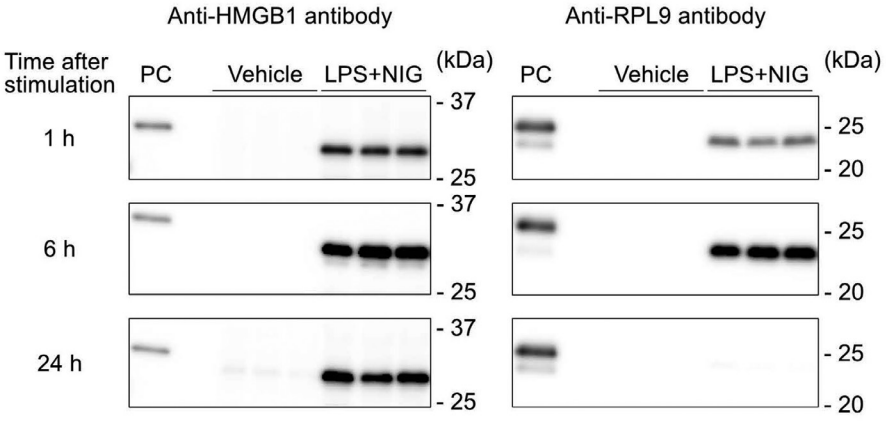

Fig. 1. Time-Course Analysis of the HMGB1 and RPL9 Release from LPS and NIG-Stimulated THP-1 Cells

The cells were stimulated with vehicle or 100 ng/mL LPS and 10 μM NIG. The culture supernatant was collected at 1, 6, and 24 h after stimulation, and then analyzed by Western blotting to detect HMGB1 (~25 kDa) and RPL9 (~22 kDa). In each blot, 100 ng/lane of recombinant HMGB1 and RPL9 was loaded (positive control, PC). Data from three independent experiments are shown. Total protein staining of the membranes is shown in Supplementary Fig. 1.

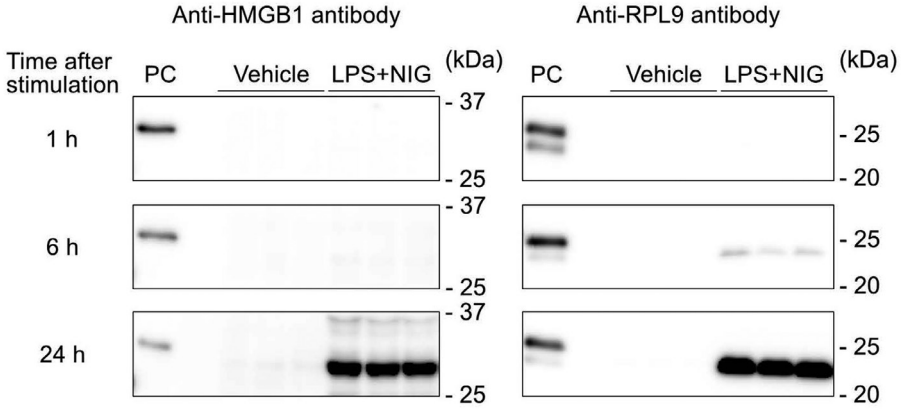

Fig. 2. Time-Course Analysis of the HMGB1 and RPL9 Release from LPS and NIG-Stimulated HepG2 Cells

The cells were stimulated with vehicle or 100 ng/mL LPS and 10 μM NIG, and then analyzed as described in Fig. 1. Total protein staining of the membranes is shown in Supplementary Fig. 2.

cells, a human liver cell model, were examined under the same conditions as THP-1 cells. At 1 h after stimulation, HMGB1 and RPL9 were barely detectable (Fig. 2), although a slight amount of RPL9 was detected in the culture supernatant of the stimulated cells with a prolonged exposure time during chemiluminescence detection (data not shown). The release of RPL9 became more evident at 6 h, whereas HMGB1 remained difficult to detect. The amount of RPL9 significantly increased at 24 h, and HMGB1 became detectable at a comparable level to RPL9.

In addition, a similar analysis was performed using EA.hy926 cells, a human endothelial cell model. In contrast to THP-1 and HepG2, the release of HMGB1 and RPL9 from stimulated EA.hy926 cells was not observed at 1 or 6 h (Fig. 3). At 24 h, the proteins were only detectable at a minimal level.

Comparison of the GSDMD Cleavage among LPS and NIG-Stimulated THP-1, HepG2, and EA.hy926 Cells Based on these results, we next investigated whether pyroptosis was induced in the tested cells. GSDMD cleavage, a key process of pyroptosis, was compared among the stimulated cells at each time point (Fig. 4). The stimulation condition was set to induce pyroptosis in THP-1 cells. In THP-1 cells, bands representing full-length and cleaved GSDMD were detected at 1 and 6 h after LPS and NIG addition. At 24 h, only a weak band representing cleaved GSDMD was observed, and the full-length band was barely detectable. Unlike THP-1, cleaved GSDMD was not detected in stimulated HepG2 or EA.hy926 cells. However, at 24 h, a decrease or disappearance of the full-length GSDMD band was observed in HepG2 and EA.hy926 cells.

Comparison of the Cell Viability under Stimulated Conditions Considering that pyroptosis was induced only in THP-1 cells, we performed additional experiments to compare the cellular state under stimulated conditions. First, we compared the viability of each cell line at different time points by MTS assay (Fig. 5). The viability of stimulated THP-1 cells decreased to 54% compared with vehicle-stimulated cells at 1 h, and significantly decreased to less than 30% at 6 and 24 h, indicating the progression of pyroptosis. The viability of HepG2 cells also decreased to 56% at 1 h, but remained at the same level for up to 6 h; then, it significantly reduced to less than 30% at 24 h. Conversely, the viability of EA.hy926 cells

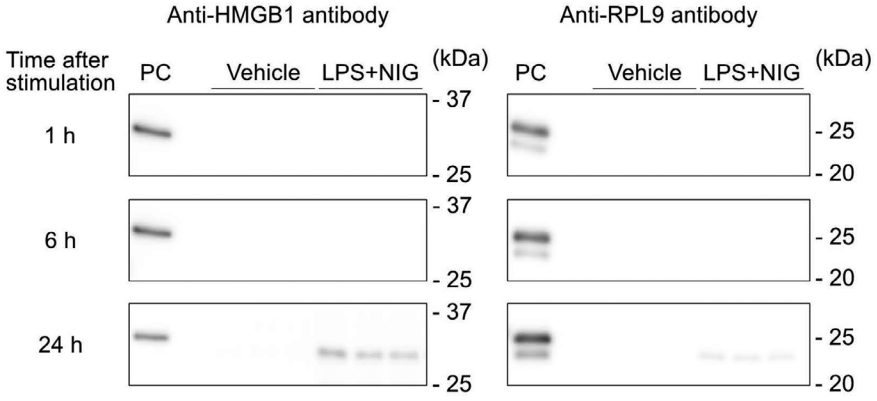

Fig. 3. Time-Course Analysis of the HMGB1 and RPL9 Release from LPS and NIG-Stimulated EA.hy926 Cells

The cells were stimulated with vehicle or 100 ng/mL LPS and 10 μM NIG, and then analyzed as described in Fig. 1. Total protein staining of the membranes is shown in Supplementary Fig. 3.

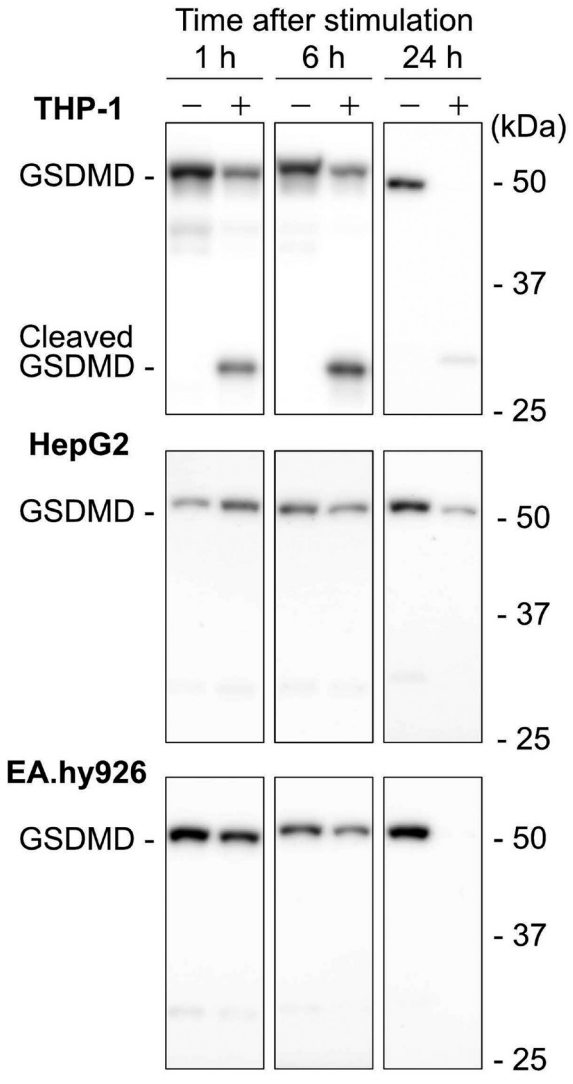

Fig. 4. Comparison of GSDMD Cleavage among LPS and NIG-Stimulated THP-1, HepG2, and EA.hy926 Cells

The cells were stimulated with vehicle (−) or 100 ng/mL LPS and 10 μM NIG (+). Whole cells were harvested at 1, 6, or 24 h after stimulation, and then analyzed by Western blotting to detect GSDMD (~53 kDa) and its cleaved form (~30 kDa). In each lane, 25 μg of cellular proteins were loaded. Representative data from three independent experiments are shown. Total protein staining of the membranes is shown in Supplementary Fig. 4.

remained above 80% for up to 6 h, and decreased to 30% at 24 h.

Comparison of the Cell Death Patterns under Stimulated Conditions Although the viability of all three cell lines decreased similarly within 24 h, the time-dependent differences in their viability patterns suggest that distinct forms of cell death occurred. To investigate these differences, we compared the cell death patterns by monitoring the integrity of the cellular membranes over time, specifically the externalization of PS and the exposure of nuclear DNA (Fig. 6). In THP-1 cells, luminescent signals representing the amount of PS exposed on the cell surface significantly increased between 6 and 24 h, indicating the loss of membrane asymmetry associated with the progression of cell death. The fluorescent signals representing the exposure of nuclear DNA significantly increased after 2 h, but no significant increase was observed thereafter. Similar to THP-1 cells, luminescent signals in HepG2 cells significantly increased between 6 and 24 h. However, unlike THP-1 cells, fluorescent signals in HepG2 cells significantly increased between 6 and 20 h. In EA.hy926 cells, luminescent signals did not significantly change during the observation period. Similar to HepG2 cells, fluorescent signals in EA.hy926 cells significantly increased between 20 and 24 h.

DISCUSSION

The central hypothesis of this study was that the release kinetics differ between HMGB1, a pro-inflammatory DAMP, and RPL9, a candidate regulatory DAMP, providing a mechanism to explain how HMGB1's activity can manifest despite the co-release of its potential inhibitor. Our results support this hypothesis and reveal that time-dependent regulation is highly cell-type specific. The differential temporal release of these molecules was observed, which may play an important role in maintaining immune homeostasis *in vivo*.

In THP-1 macrophages, we observed a rapid, sequential release pattern consistent with their role as first responders. The initial phase (1 h) was marked by the predominant release of HMGB1, ensuring the rapid initiation of an inflammatory alarm. This was followed by a second phase (6 h), where RPL9 release increased to a comparable level as pyroptosis progressed, thereby serving to control the initial response (Fig. 1). In contrast, the delayed and staggered release of the

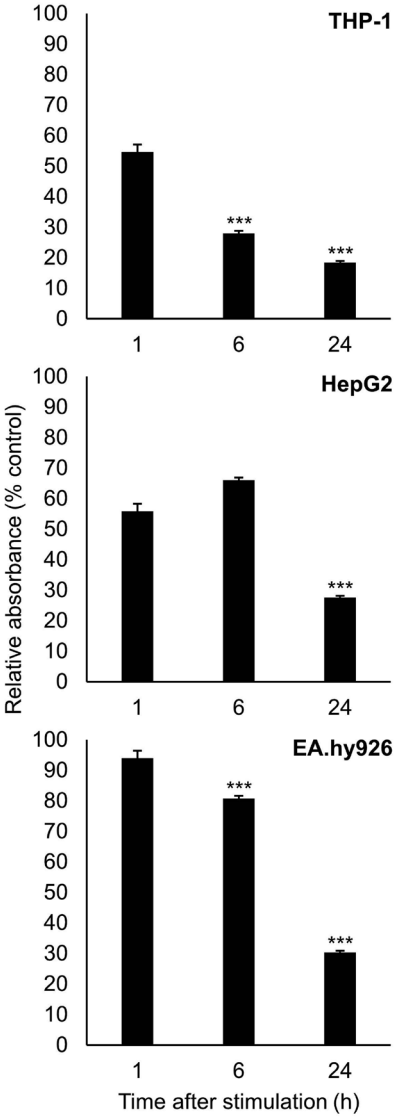

Fig. 5. Comparison of the Cellular Viability among the LPS and NIG-Stimulated THP-1, HepG2, and EA.hy926 Cells

The cells were stimulated with 100 ng/mL LPS and 10 μM NIG. At 1, 6, or 24 h after stimulation, the medium containing LPS and NIG was replaced with fresh medium containing the viability assay compound, and the cells were incubated for 3 h. After incubation, the amount of formazan product metabolized from the compound in living cells was estimated by measuring its absorbance at 492 nm. At each time point, the absorbance of the cells stimulated with LPS and NIG was shown relative to that of the cells stimulated with vehicle. ***, $P < 0.001$ indicates a significant difference from the 1 h time point using Dunnett's test (n = 4).

two DAMPs from HepG2 liver cells suggested a self-protective strategy. The earlier release of inhibitory protein RPL9 observed at 6 h, long before the appearance of a significant level of HMGB1, would precondition the local environment to reduce subsequent inflammatory damage (Fig. 2). This unique protective mechanism may be particularly important for the liver because it is anatomically positioned to be constantly exposed to gut-derived LPS via the portal vein. Meanwhile, the profound resistance of EA.hy926 endothelial cells to the stimulus (Fig. 5) is consistent with their critical role in both regulating inflammation and maintaining the vascular barrier. This resistance to lytic cell death is likely essential to prevent systemic spillover (Fig. 3).

Our cell death analysis strongly supports the mechanistic basis for these distinct release patterns, revealing that the timing of passive release is caused by different underlying forms of regulated cell death. The rapid passive release from THP-1 cells was a direct consequence of classical pyroptosis, as demonstrated by the early detection of cleaved GSDMD (Fig. 4), the sharp decrease in cell viability within the first hour (Fig. 5), and the concomitant rapid exposure of nuclear DNA through GSDMD pores (Fig. 6).[15,16] Conversely, the delayed passive release of HMGB1 from HepG2 cells is consistent with secondary necrosis following an apoptosis-like process. It has been reported that HMGB1 is not released during apoptosis, but rather during the subsequent secondary necrosis.[17] This is supported by the absence of GSDMD cleavage (Fig. 4), a distinct pattern of cell viability loss (Fig. 5), and the detection of nuclear DNA exposure only at 24 h (Fig. 6), indicating that membrane integrity was maintained for an extended period before the onset of secondary necrosis (Fig. 6).[18]

Further examination of the 24 h time point revealed additional layers of regulation that clearly differed between cell types. In THP-1 cells, the transient nature of the RPL9 signal, which disappeared while the pro-inflammatory HMGB1 was still present, is noteworthy (Fig. 1). This disappearance may not be an actively regulated event, but rather a secondary consequence of the intense pyroptotic environment. One possibility is degradation by proteases released from the THP-1 cells themselves. This may include enzymes that are actively secreted proteases, such as matrix metalloproteinases,[19] or intracellular proteases like cathepsins that are passively released upon pyroptotic cell lysis.[20] Another possibility is functional consumption, in which RPL9 is cleared after binding to its targets, such as HMGB1 or LPS, to exert its inhibitory effects. Regardless of the precise mechanism, the functional outcome is the removal of an inhibitory "brake," which may allow for a sustained or secondary wave of inflammation driven by the persistent HMGB1. Notably, the situation in HepG2 cells at 24 h appears to represent a different endpoint. The preceding release of RPL9 can be interpreted as an initial protective attempt. However, the substantial release of both HMGB1 and RPL9 at 24 h is likely the consequence of widespread secondary necrosis, indicating that this protective effort is ultimately insufficient (Fig. 2). These differences suggest that the extracellular space is a dynamic environment where DAMP levels are governed by a complex, cell-type-specific balance of release, degradation, and clearance.

Notably, we identified a temporal association between the externalization of PS (Fig. 6) and the release of RPL9 (Figs. 1 and 2). This phenomenon is common to both THP-1 and HepG2 cells, despite their different primary cell death pathways. This suggests the existence of a selective release pathway for RPL9 that is linked to early membrane reorganization events, such as PS externalization,[21] and does not require complete cell lysis. Extracellular vesicles (EVs), which are released during membrane reorganization, are a plausible candidate for mediating this selective release.[22] This possibility is consistent with our sample preparation because the centrifugation protocol would enrich smaller EVs while removing larger debris and apoptotic bodies.

The concept of an EV-mediated release raises new questions about the extracellular function of RPL9. While further investigation is required, this model does not preclude RPL9's inhibitory function. For example, considering that EVs pre-

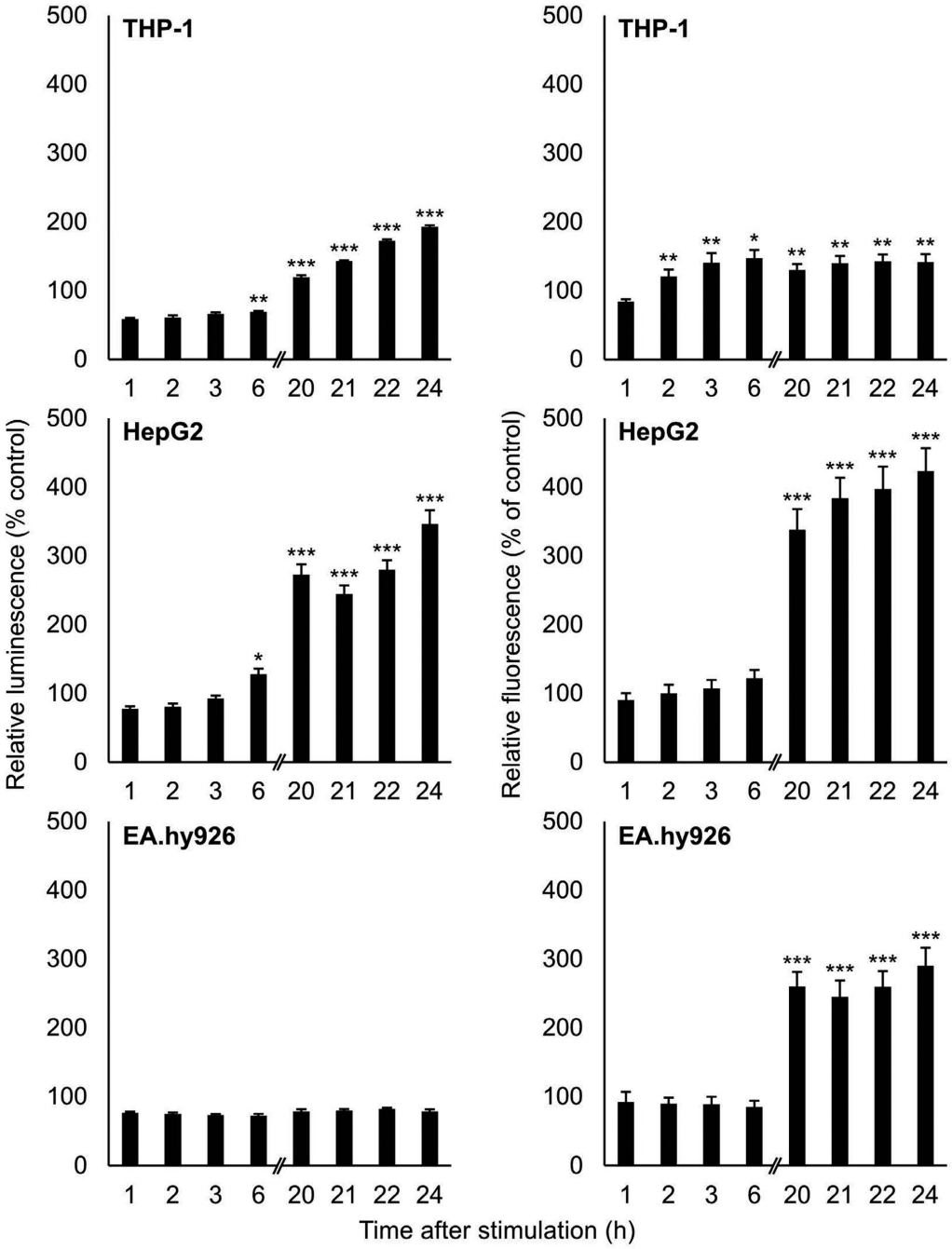

Fig. 6. Comparison of the Cell Death Patterns among the LPS and NIG-Stimulated THP-1, HepG2, and EA.hy926 Cells

The cells were stimulated with 100 ng/mL LPS and 10 μM NIG in the presence of the detection reagent for phosphatidylserine (PS) and DNA. At each point from 1 to 24 h after stimulation, a luminescent signal reflecting PS exposure to the extracellular space and a fluorescent signal reflecting DNA exposure were measured in each well. At each time point, luminescent and fluorescent signals of the cells stimulated with LPS and NIG were shown relative to those of the cells stimulated with vehicle. *, $P < 0.05$; **, $P < 0.01$; ***, $P < 0.001$ indicates a significant difference from the 1 h time point using Dunnett's test (n = 4).

sent various molecules derived from their parent cells on their surface,[23] RPL9 presented on the surface of EVs may act as a high-density decoy for HMGB1 or LPS. Alternatively, given that the integrity of EVs is influenced by the microenvironment,[23] EVs may release their cargo in response to specific environmental cues such as the low pH or high protease activity at inflammatory sites. Although these possibilities are speculative, the elucidation of this selective release pathway for RPL9 represents a critical future direction for understanding the function of regulatory DAMPs.

In conclusion, this study demonstrates that the regulation of DAMP-mediated inflammation depends not only on which molecules are released but also on when and how they are released. Despite its *in vitro* nature, our work reveals a complex, cell-type-specific temporal control system and suggests the existence of a novel, selective release pathway for RPL9. Understanding these time-dependent regulatory processes is essential for developing new therapeutic strategies that can finely tune the inflammatory response.

Funding This study was supported by the Japan Society for the Promotion of Science (JSPS) KAKENHI [grant numbers 24K09905, 24K09973] and the Ryobi Teien Memory Foundation.

Conflict of interest The authors declare no conflict of interest.

REFERENCES

1) Lotze MT, Tracey KJ. High-mobility group box 1 protein (HMGB1): nuclear weapon in the immune arsenal. *Nat. Rev. Immunol.*, **5**, 331–342 (2005).
2) Bianchi ME. DAMPs, PAMPs and alarmins: all we need to know about danger. *J. Leukoc. Biol.*, **81**, 1–5 (2007).
3) Gong T, Liu L, Jiang W, Zhou R. DAMP-sensing receptors in sterile inflammation and inflammatory diseases. *Nat. Rev. Immunol.*, **20**, 95–112 (2020).
4) van Beijnum JR, Buurman WA, Griffioen AW. Convergence and amplification of toll-like receptor (TLR) and receptor for advanced glycation end products (RAGE) signaling pathways via high mobility group B1 (HMGB1). *Angiogenesis*, **11**, 91–99 (2008).
5) Youn JH, Kwak MS, Wu J, Kim ES, Ji Y, Min HJ, Yoo J-H, Choi JE, Cho H-S, Shin J-S. Identification of lipopolysaccharide-binding peptide regions within HMGB1 and their effects on subclinical endotoxemia in a mouse model. *Eur. J. Immunol.*, **41**, 2753–2762 (2011).
6) Watanabe M, Toyomura T, Tomiyama M, Wake H, Liu K, Teshigawara K, Takahashi H, Nishibori M, Mori S. Advanced glycation end products (AGEs) synergistically potentiated the proinflammatory action of lipopolysaccharide (LPS) and high mobility group box-1 (HMGB1) through their direct interactions. *Mol. Biol. Rep.*, **47**, 7153–7159 (2020).
7) Watanabe M, Toyomura T, Wake H, Nishinaka T, Hatipoglu OF, Takahashi H, Nishibori M, Mori S. Identification of ribosomal protein L9 as a novel regulator of proinflammatory damage-associated molecular pattern molecules. *Mol. Biol. Rep.*, **49**, 2831–2838 (2022).
8) Chen R, Kang R, Tang D. The mechanism of HMGB1 secretion and release. *Exp. Mol. Med.*, **54**, 91–102 (2022).
9) He WT, Wan H, Hu L, Chen P, Wang X, Huang Z, Yang Z-H, Zhong C-Q, Han J. Gasdermin D is an executor of pyroptosis and required for interleukin-1β secretion. *Cell Res.*, **25**, 1285–1298 (2015).
10) Volchuk A, Ye A, Chi L, Steinberg BE, Goldenberg NM. Indirect regulation of HMGB1 release by gasdermin D. *Nat. Commun.*, **11**, 4561 (2020).
11) Begum S, Moreau F, Leon Coria A, Chadee K. Entamoeba histolytica stimulates the alarmin molecule HMGB1 from macrophages to amplify innate host defenses. *Mucosal Immunol.*, **13**, 344–356 (2020).
12) Mariathasan S, Weiss DS, Newton K, McBride J, O'Rourke K, Roose-Girma M, Lee WP, Weinrauch Y, Monack DM, Dixit VM. Cryopyrin activates the inflammasome in response to toxins and ATP. *Nature*, **440**, 228–232 (2006).
13) Watanabe M, Toyomura T, Wake H, Liu K, Teshigawara K, Takahashi H, Nishibori M, Mori S. Advanced glycation end products attenuate the function of tumor necrosis factor-like weak inducer of apoptosis to regulate the inflammatory response. *Mol. Cell. Biochem.*, **434**, 153–162 (2017).
14) Liu K, Mori S, Takahashi HK, Tomono Y, Wake H, Kanke T, Sato Y, Hiraga N, Adachi N, Yoshino T, Nishibori M. Anti-high mobility group box 1 monoclonal antibody ameliorates brain infarction induced by transient ischemia in rats. *FASEB J.*, **21**, 3904–3916 (2007).
15) Shi J, Zhao Y, Wang K, Shi X, Wang Y, Huang H, Zhuang Y, Cai T, Wang F, Shao F. Cleavage of GSDMD by inflammatory caspases determines pyroptotic cell death. *Nature*, **526**, 660–665 (2015).
16) Kovacs SB, Miao EA. Gasdermins: effectors of Pyroptosis. *Trends Cell Biol.*, **27**, 673–684 (2017).
17) Scaffidi P, Misteli T, Bianchi ME. Release of chromatin protein HMGB1 by necrotic cells triggers inflammation. *Nature*, **418**, 191–195 (2002).
18) Galluzzi L, Vitale I, Aaronson SA, Abrams JM, Adam D, Agostinis P, Alnemri ES, Altucci L, Amelio I, Andrews DW, Annicchiarico-Petruzzelli M, Antonov AV, Arama E, Baehrecke EH, Barlev NA, Bazan NG, Bernassola F, Bertrand MJM, Bianchi K, Blagosklonny MV, Blomgren K, Borner C, Boya P, Brenner C, Campanella M, Candi E, Carmona-Gutierrez D, Cecconi F, Chan FK-M, Chandel NS, Cheng EH, Chipuk JE, Cidlowski JA, Ciechanover A, Cohen GM, Conrad M, Cubillos-Ruiz JR, Czabotar PE, D'Angiolella V, Dawson TM, Dawson VL, De Laurenzi V, De Maria R, Debatin K-M, DeBerardinis RJ, Deshmukh M, Di Daniele N, Di Virgilio F, Dixit VM, Dixon SJ, *et al*. Molecular mechanisms of cell death: recommendations of the Nomenclature Committee on Cell Death 2018. *Cell Death Differ.*, **25**, 486–541 (2018).
19) Yang C-C, Lin C-C, Hsiao L-D, Kuo J-M, Tseng H-C, Yang C-M. Lipopolysaccharide-Induced Matrix Metalloproteinase-9 Expression Associated with Cell Migration in Rat Brain Astrocytes. *Int. J. Mol. Sci.*, **21**, 259 (2019).
20) Li Q, Falkler WA Jr, Bever CT Jr. Endotoxin induces increased intracellular cathepsin B activity in THP-1 cells. *Immunopharmacol. Immunotoxicol.*, **19**, 215–237 (1997).
21) Nagata S, Suzuki J, Segawa K, Fujii T. Exposure of phosphatidylserine on the cell surface. *Cell Death Differ.*, **23**, 952–961 (2016).
22) Caruso S, Poon IKH. Apoptotic Cell-Derived Extracellular Vesicles: More Than Just Debris. *Front. Immunol.*, **9**, 1486 (2018).
23) van Niel G, D'Angelo G, Raposo G. Shedding light on the cell biology of extracellular vesicles. *Nat. Rev. Mol. Cell Biol.*, **19**, 213–228 (2018).